ACS OMEGA

http://pubs.acs.org/journal/acsodf

Article

Removal of Methylene Blue Dye from Aqueous Solutions by Pullulan Polysaccharide/Polyacrylamide/Activated Carbon Complex Hydrogel Adsorption

Kewei Chen, Yanhui Li,* Mingzhen Wang, Qiuju Du, Yaohui Sun, Yang Zhang, Bing Chen, Zhenyu Jing, Yonghui Jin, and Shiyong Zhao

Cite This: *ACS Omega* 2023, 8, 857−867

Read Online

ACCESS | Metrics & More | Article Recommendations

ABSTRACT: In this study, composite hydrogels were prepared using a simple synthetic technique to adsorb methylene blue (MB) from water. The hydrogel comprised potassium persulfate (KPS) as the initiator, *N*,*N*′-methylene bisacrylamide as the crosslinking agent, and sodium hydroxide (NaOH) as the activator. It was employed to adsorb MB at different concentrations from water. The morphology and properties of PUL/PAM/GO composites were characterized through thermogravimetric analysis, Fourier transform infrared spectroscopy, and scanning electron microscopy. Moreover, the adsorption properties, adsorption isotherms, adsorption kinetics, adsorption thermodynamics, and swelling properties of the hydrogel for MB were investigated. The optimal ratio of PUL to AC was obtained as 6:1 by fixing the amount of PUL and loading AC of different masses. The maximum adsorption capacity was obtained as 591.4 mg/g. It also exhibited certain mechanical strength. The adsorption of MB conforms to pseudo-first-order kinetics and Langmuir isotherms. In this study, an environment-friendly, cheap, simple, and efficient way was presented for the composite hydrogel in the direction of water treatment.

INTRODUCTION

With the increase of organic dyes in the environment, organic dye pollution has become a major component of environmental pollution over the past few decades. Dyes are not biodegradable for their complex aromatic structure such that wastewater containing excess dyes should be treated before it can be discharged into natural water. Even small amounts of dye in water can cause serious water pollution problems.

Methylene blue (MB) is a cationic dye that has been extensively employed in people's daily lives. If MB is excessively used and not effectively removed, human tissue necrosis, high blood pressure, quadriplegia, and other human diseases will be caused after MB reaches the human body through the food chain.[1,2] The removal of MB using a cheap adsorbent has been confirmed as an internationally recognized efficient and environment-friendly dye adsorption method, which is capable of minimizing the pollution of MB to the environment.[3−7] Accordingly, exploring cheap and efficient adsorbents becomes the focus of research.

Hydrogels, as a hot field, have been popular in disciplines (e.g., pharmacy, biomedicine, and chemical industry).[8−10] Compared with other adsorbents, hydrogels exhibit higher water content, can be adjusted by biochemistry, and have certain mechanical properties and biocompatibility.[11−14] Researchers have investigated hydrogels loaded with polysaccharides (e.g., guar gum, chitosan, and cellulose) to obtain superior properties of hydrogels for drug delivery, soft tissue engineering, and other fields.[15−17]

Pullulan polysaccharide (PUL), a common and cheap polysaccharide in people's daily life, has been extensively explored and aroused wide attention for its excellent biocompatibility and pollution-free material.[18] PUL has been

Received: September 27, 2022
Accepted: December 8, 2022
Published: December 20, 2022

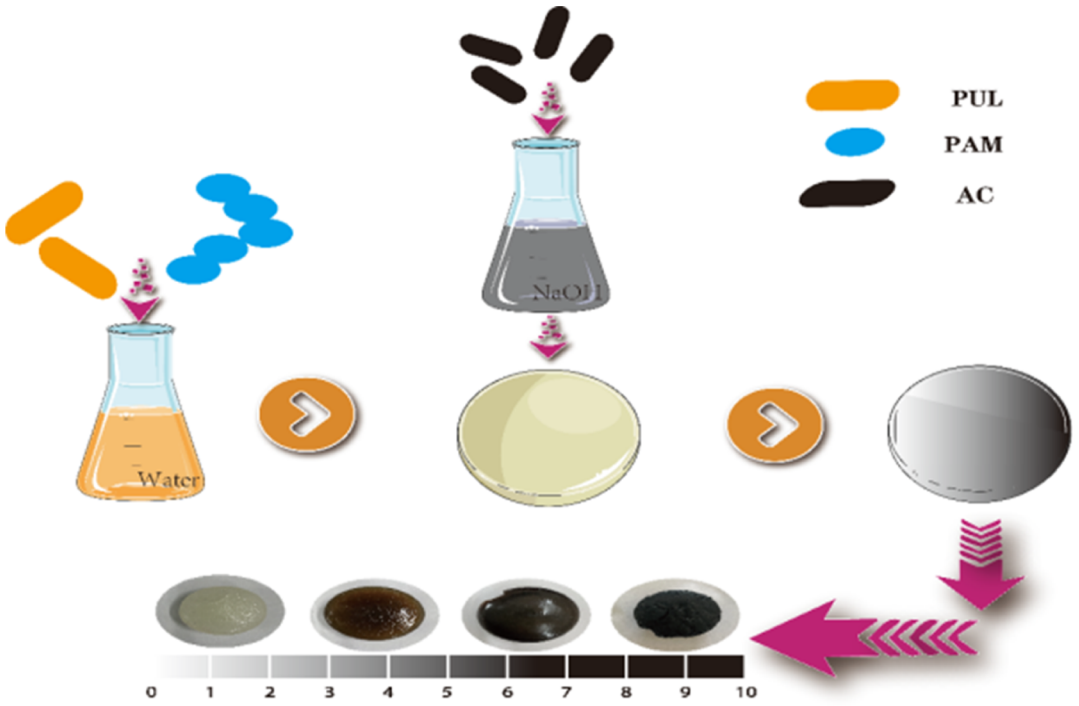

Figure 1. Schematic diagram of preparation of PUL/PAM/AC.

employed in food thickeners, capsule bonding molding agents, water-soluble packaging materials, adsorption materials, and other fields, with broad application prospects.[19−21]

Activated carbon (AC) for agriculture and forestry waste and carbon materials (e.g., coal resources through high-temperature carbonization and activation) exhibit good chemical inertness, rich functional groups, and the advantages of wide raw material sources. Besides, the AC powder disperses well in water. It is necessary to find low-cost carriers and biodegradable materials to fix AC to prevent further pollution by aqueous solution.[22−24]

Most of the hydrogels exhibit poor mechanical strength and low adsorption capacity, and they are not recycled. Polyacrylamide (PAM), a type of tenacious hydrogel matrix, is capable of endowing hydrogels with certain mechanical strength and adsorption characteristics, providing the active site for powdery AC to adsorb pollutants, facilitating the adsorption process.[25−27]

In this study, PUL/PAM/AC hydrogels with different AC concentrations were innovatively prepared, thus effectively solving the problems of AC dispersing in water. Moreover, the prepared hydrogels exhibited certain swelling and mechanical properties, and the ability of composite material to treat wastewater was significantly improved. The physical and chemical properties and surface morphology of the hydrogel were characterized. The adsorption properties of the hydrogel for MB were systematically investigated. The method presented in this study provides a more environment-friendly and low-cost way for the hydrogel adsorption of MB.

MATERIAL AND METHODS

Reagents and Materials. All chemicals are used directly upon purchase without handling. MB (AR) was purchased from Tianjin Guangcheng Chemical Reagent Co., Ltd., China. Sodium hydroxide (NaOH) (AR) was purchased from Sinopharm Chemical Reagent Co., Ltd., China. BIS ($C_7H_{10}N_2O_2$, 97%), AM (C_3H_5NO, 98%), KPS ($K_2S_2O_8$, 99%), and PUL $(C_{37}H_{62}O_{30})_n$ were purchased from Henan Wanbang Chemical Technology Co., Ltd., China. AC (95%) was purchased from Qingdao Hairui Co., Ltd., China.

Synthesis of the Hydrogel. PUL/PAM/AC composite hydrogels were prepared by solution polymerization, as shown in Figure 1.[28] AC with different mass ratios was added into 20 mL of NaOH with 20% mass fraction and treated with ultrasonic waves for 30 min. 0.5 g of PUL was added to the solution at a slow interval, and the mixed solution was stirred using a magnetic stirrer at a constant speed for 24 h. AM, BIS, and KPS were added to deionized water according to the previous steps and mixed with PUL/PAM for 2 min. Then, the mixture was subjected to vacuum drying at 353 K for 24 h to obtain PUL/PAM/AC composite hydrogel material. 2.364 g of PUL/PAM/AC hydrogel was heated in a box electric oven at 383 K in vacuum until the water was completely lost. The sample was 0.1546 g, with 94.5% water loss.

Characterization. The surface morphologies of PUL/PAM, AC, and PUL/PAM/AC (with different AC contents) composites were characterized by scanning electron microscopy (SEM) (Supra 55, Zeiss, Germany). The thermal stability was measured by thermogravimetric analysis (TGA) (SDT 650, Waters, Germany) ranging from 30 to 700 °C. The surface functional groups of different materials were tested using a spectrometer at 400−3500 cm^{-1} wavenumber. The specific surface area was calculated using an automated surface analyzer at 77 K.

MB Adsorption Studies. The adsorption capacities of MB on samples with different concentrations of AC were compared. In order to evaluate the adsorption performance of hydrogels at the optimum AC concentration, batch dye adsorption experiments were performed, including dose, temperature, contact time, and pH. The concentration of MB used in this experiment is 0.3 g/L. The whole adsorption experiment was carried out in a temperature-controlled gas

https://doi.org/10.1021/acsomega.2c06205
ACS Omega 2023, 8, 857−867

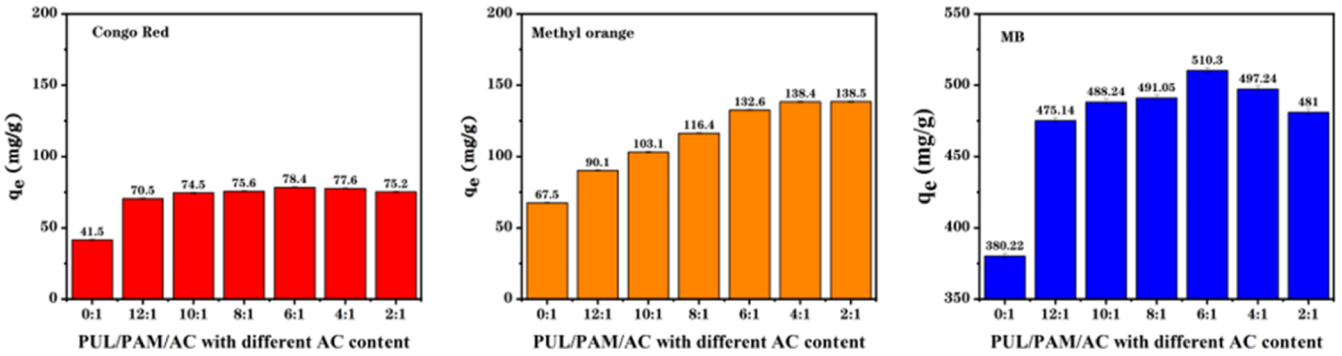

Figure 2. Adsorption of MB, Congo red, and methyl orange by different AC contents of PUL/PAM/AC.

bath vibrator at a rate of 180 rpm. The formulas are as follows:[29,30]

$$q_e = \frac{(c_0 - c_e)}{m} \times V \quad (1)$$

$$E = \frac{c_0 - c_t}{c_0} \times 100\% \quad (2)$$

where c_0 (g/L), c_e (g/L), c_t (g/L), and q_e (mg·g^{-1}) are the initial MB concentration, the final MB concentration, the MB concentration at time t (min), and the adsorption capacity, respectively. Solution volume and adsorbent mass are expressed as V (mL) and m (mg), respectively.

Swelling Measurements. To study the swelling properties of hydrogels with different pH values, the swelling rates of hydrogels were measured by gravimetric method,[31] according to the equal amounts of 1 g sample in different pH values of deionized water. 1 g of the same volume of samples was taken and put into deionized water with different pH values. After waiting for inflation in the medium hydrogel, the sample was taken out for the measurement. Blotting with filter paper was performed at an equal distance on the surface of the hydrogel. Subsequently, the data were measured every 2 h according to the weight. The formula is as follows[32]

$$Q_{eq} = \frac{m_1 - m_2}{m_2} \quad (3)$$

where m_1, m_2, and Q_{eq} are the weight of the swollen sample, the weight of the dry sample, and the equilibrium water adsorption, respectively.

RESULTS AND DISCUSSION

Adsorption Performance of Samples Loaded with Different AC Concentrations. PUL/PAM/AC ternary hydrogel materials loaded with different AC were prepared by controlling the proportion of PUL and AC. The effect of AC content on adsorption MB is presented in Figure 2. At the temperature of 298 K, the initial concentration of 0.3 g/L, and a constant natural pH, the effect of PUL/AC ratio on adsorption performance was studied. By studying the removal rate of 0.3 g/L Congo red dye and methyl orange dye, it was found that the highest adsorption capacity of Congo red dye was 77.6 mg/g, the highest adsorption capacity of methyl orange dye was 138.5 mg/g, and the highest adsorption capacity of MB was 591.4 mg/g. In this study, MB was continued to be selected as the adsorption material. PUL/PAM hydrogel adsorption capacity of MB was low. However, after AC was added in the hydrogel, the material adsorption capacity of MB increased significantly. With the increase of the AC concentration, the adsorption performance of the dye was gradually improved. When the ratio reached 6:1, AC was added continuously, and the adsorption capacity of PUL/PAM/AC on MB decreased. The possible reason for this result is that with the increase of AC, the internal structure of the terpolymer hydrogel material became more complicated, and the fluidity between the pores was blocked, thus affecting the adsorption performance of the material. Accordingly, the optimal adsorption ratio of 6:1 composite hydrogel was selected for subsequent experiments.

Characterization of PUL/PAM/AC. Figure 3a,b shows PUL/PAM and AC SEM images, respectively. PUL/PAM had a smooth and flat surface without significant folds, while AC exhibited a messy and rough surface structure with folds. Figure 3c,d depicts PUL/PAM/AC (PUL/AC is 10:1 and PUL/AC 6:1); PUL/PAM/AC at a low concentration of AC exhibited an obvious and wide fold structure, probably because the surface of the material became uneven after PUL/PAM wraps the AC.[33] With the increase of AC concentration, more significant fold structure appeared, as shown in Figure 3d. The area of dye molecules can be attached to increase, which can also account for the enhanced adsorption capacity of materials.

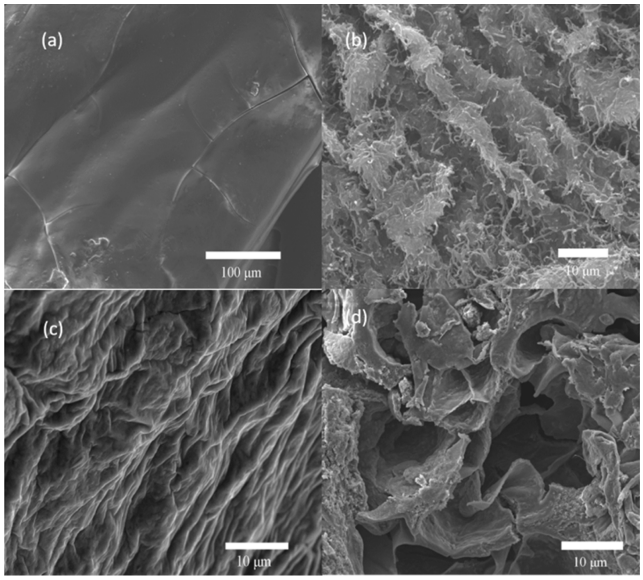

Figure 3. SEM images of PUL/PAM (a), AC (b), and PUL/PAM/AC with different AC contents (c,d).

https://doi.org/10.1021/acsomega.2c06205
ACS Omega 2023, 8, 857−867

Fourier transform infrared (FTIR) analysis in Figure 4 was conducted to gain insights into the distribution of functional groups on the surface of composites. The vibration of PUL at 1020 cm^{-1} and PUL/PAM/AC at 1050 cm^{-1} was considered stretching of C−O−C, and the existence of PUL was observed.[34] The vibration of PAM and PUL/PAM/AC at 2940 cm^{-1} was an aliphatic tensile peak, accounting for the presence of PAM in the material.[35] The peaks of AC at 833 cm^{-1} and PUL/PAM/AC at 880 cm^{-1} belonged to C−H transverse bending vibration of CH═N group, and the peaks of PUL/PAM/AC at 1410 and 1560 cm^{-1} belonged to C−OH tensile vibration and C═C stretching vibration, respectively.[36] In the infrared spectra of PUL, PAM, and AC, the peaks all existed in PUL/PAM/AC, thus indicating the successful synthesis of the material.

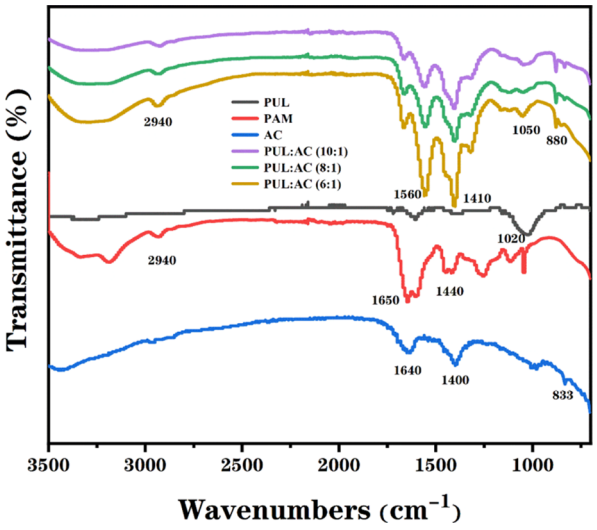

Figure 4. FTIR spectra of PUL/PAM/AC (different AC contents), PUL, PAM, and AC.

Figure 5 presents the thermal decomposition curves of PUL/PAM/AC (a) and PUL/PAM/AC with different AC contents (b). In Figure 5a, 15% weight loss at temperatures from 0 to 180 °C was attributed to the evaporation of residual water from the material. A drop in the curve (14%) was identified in the temperature range of 180−400 °C, probably due to the decomposition of protein and the polymer PAM. Another sharp drop in mass (17%) at 400−700 °C was attributed to the decomposition of oxygen-containing functional groups on the surface of carbohydrates (e.g., PUL polysaccharides and ACs).[37−39] The TGA curve indicated that the total mass loss of PUL/PAM/AC was nearly 46%, and no significant mass loss occurred after 500 °C, thus suggesting that the material exhibits good stability. As depicted in Figure 5b, with the increase of AC content, the mass loss of the material was reduced. Under the inert gas, the material was stable in the form of carbon.

The specific surface areas of PUL/PAM and PUL/PAM/AC were determined by N_2 adsorption isotherms. In Figure 6a, BET calculates that the specific surface area of PUL/PAM/AC (PUL/AC 6:1) was 1.85 $m^2 \cdot g^{-1}$, which was less than the specific surface area of PUL/PAM of 2.73 $m^2 \cdot g^{-1}$. The specific surface area tends to decrease with the increase of AC concentration, which was due to the local phase transformation of materials caused by the addition of AC in the chaotic ternary system network, resulting in partial loss of surface structure and the decrease of specific surface area.[40] Figure 6b shows that the pore sizes of PUL/PAM/AC (PUL/AC 6:1) were mainly 23.41, 27.34, and 40.03 Å, confirming that the material was a mesoporous material.

Effects of pH, Dose, Temperature, and Contact Time. Figure 7 shows the effect of dose on the adsorption effect. With the increase of adsorbent dose, the removal rate of MB increased, which is mainly because the increase of adsorbent surface active sites can affect the removal rate. When the amount of adsorbent increased, although the adsorption capacity continued to increase, the removal rate of MB by PUL/PAM/AC increased no longer significantly since the utilization rate of adsorption sites decreased, and excessive adsorption sites did not contribute to saturated adsorption.[41]

Figure 8a presents the effect of pH control in the range of 2−10 on adsorption properties. The curve indicated that under acidic conditions, the removal rate of MB decreased significantly. Moreover, with the gradual increase of acidic pH to natural pH, the removal rate tended to increase, and the adsorption effect was stable under alkaline pH. Under acidic conditions, the reduced adsorption efficiency can be attributed

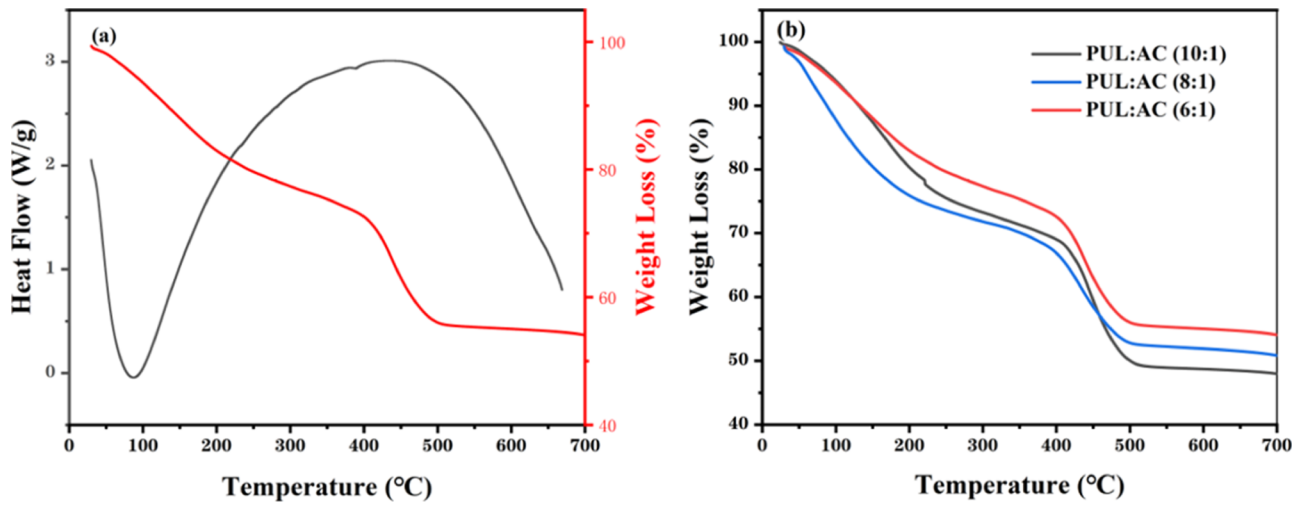

Figure 5. TGA curves of PUL/PAM/AC (6:1) (a); PUL/PAM/AC with different AC contents (b).

https://doi.org/10.1021/acsomega.2c06205
ACS Omega 2023, 8, 857−867

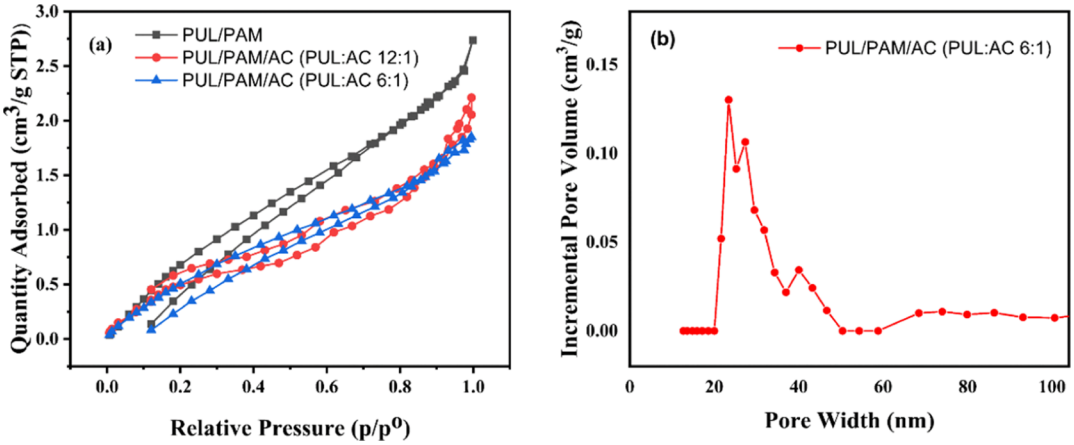

Figure 6. N_2 adsorption−desorption isotherms of PUL/PAM/AC with different AC contents (a); pore size distributions of PUL/PAM/AC (PUL/AC 6:1) (b).

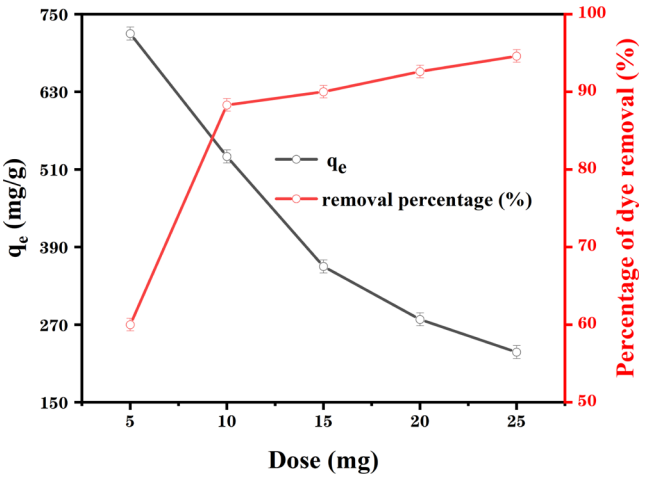

Figure 7. Effect of dose on MB onto PUL/PAM/AC.

to the presence of considerable H^+ in the solution in a low-pH environment, which will compete for the same adsorption site with MB to reduce the adsorption capacity. Furthermore, PUL/PAM/AC sample carboxyl and hydroxyl were protonated, and electrostatic repulsion was generated between MB cations.[42] Figure 8b shows the zeta potential of the hydrogels at different pH values. The results show that the zeta potential is more negative with the increase of pH. This indicates that the surface of the adsorbent is negatively charged, and the negatively charged surface can enhance the adsorption performance of the adsorbent for the positively charged MB cation through electrostatic attraction.

Temperature has always been an important feature determining the adsorption process. Figure 9 shows the influence of MB concentration between 0.2 and 0.4 g/L at 298−318 K. With the increase of temperature and MB concentration, the maximum adsorption capacity decreases and increases, respectively. The temperature rises from 298 to 318 K, and the maximum adsorption capacity drops from 0.568 to 0.463 g/L, which may be related to the electrostatic interaction between the material and MB molecules, and the reaction is exothermic.

Figure 10 shows the relationship between contact time and adsorption capacity. At the initial stage of adsorption (before 180 min), the adsorption capacity increased rapidly, and the adsorption sites were occupied rapidly in a short time. With the extension of time (940 min later), the adsorption sites were gradually occupied, resulting in no more adsorption sites, and the change of adsorption capacity increment became quantitative and tended to approach the equilibrium

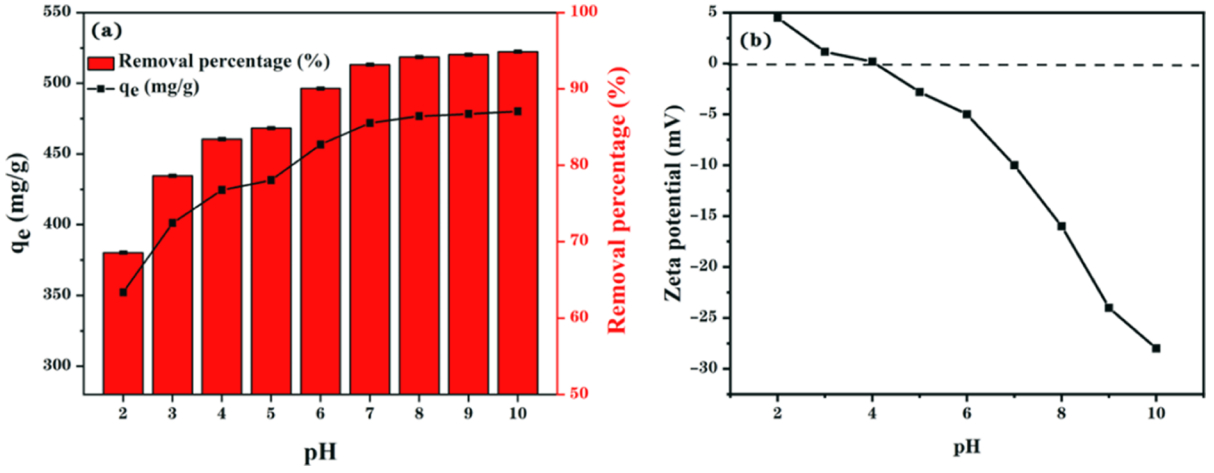

Figure 8. Effect of pH on MB onto PUL/PAM/AC (a); zeta potential (b).

https://doi.org/10.1021/acsomega.2c06205
ACS Omega 2023, 8, 857−867

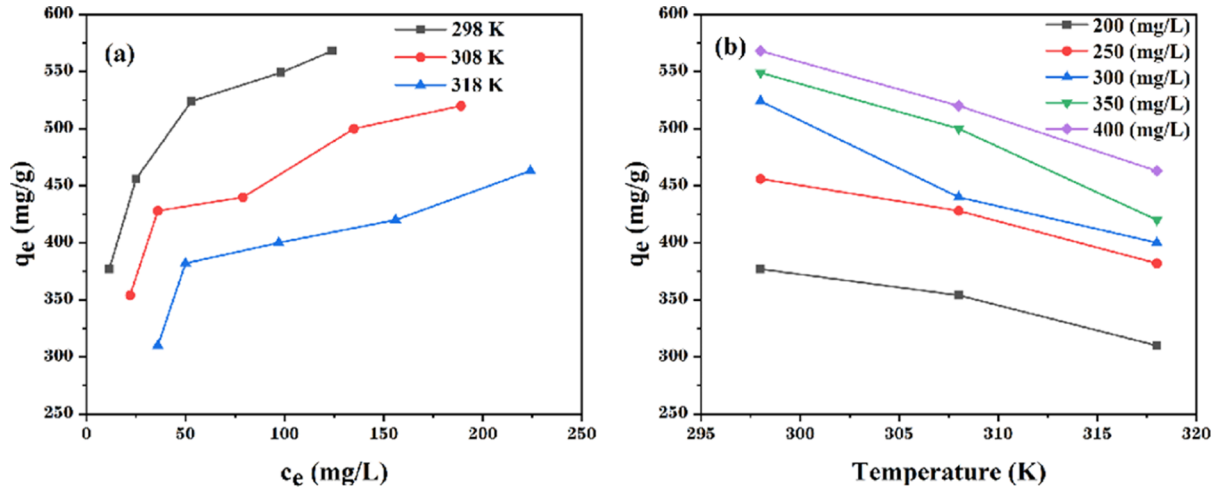

Figure 9. Effect of temperature on MB onto PUL/PAM/AC: (a) c_e and q_e and (b) temperature and q_e.

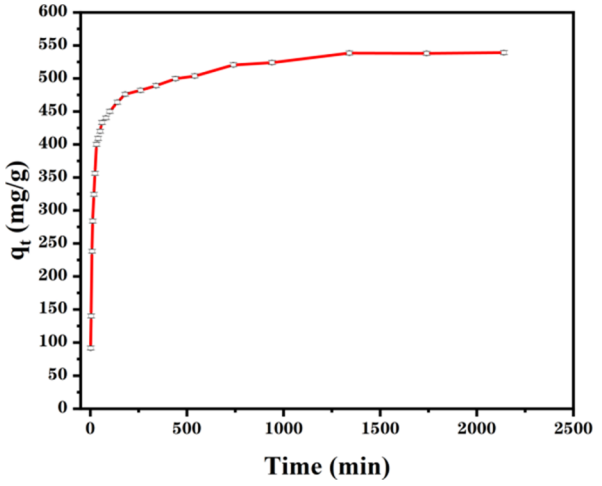

Figure 10. Effect of contact time on MB onto PUL/PAM/AC.

adsorption capacity.[43] The optimal adsorption time should be 180 min.

Adsorption Isotherm Models. An adsorption isotherm refers to adsorption equilibrium under a certain temperature, which is used to describe the relationship between the material and adsorbent adsorption interactions. The study of the adsorption isotherm is to find the mathematic expression of the adsorption capacity and adsorption conditions as well as to investigate the adsorption mechanism. More insights can be gained into the adsorption process through the theoretical model and experimental data.[44] Langmuir and Freundlich models were two commonly used models to analyze equilibrium adsorption data.

Langmuir model can be used to describe experimental results with a wide range of concentrations, assuming that adsorption only occurs on the surface and there was no interaction between adsorbents, which was a very widely used adsorption model. Langmuir adsorption isotherm model is expressed as[45,46]

$$q_e = \frac{q_m b c_e}{1 + b c_e} \tag{4}$$

where b and q_m (mg·g^{-1}) are the constants of adsorption intensity and maximum adsorption capacity, respectively.

The Freundlich model simulates multilayer adsorption, assuming that adsorption occurs at non-uniformly distributed

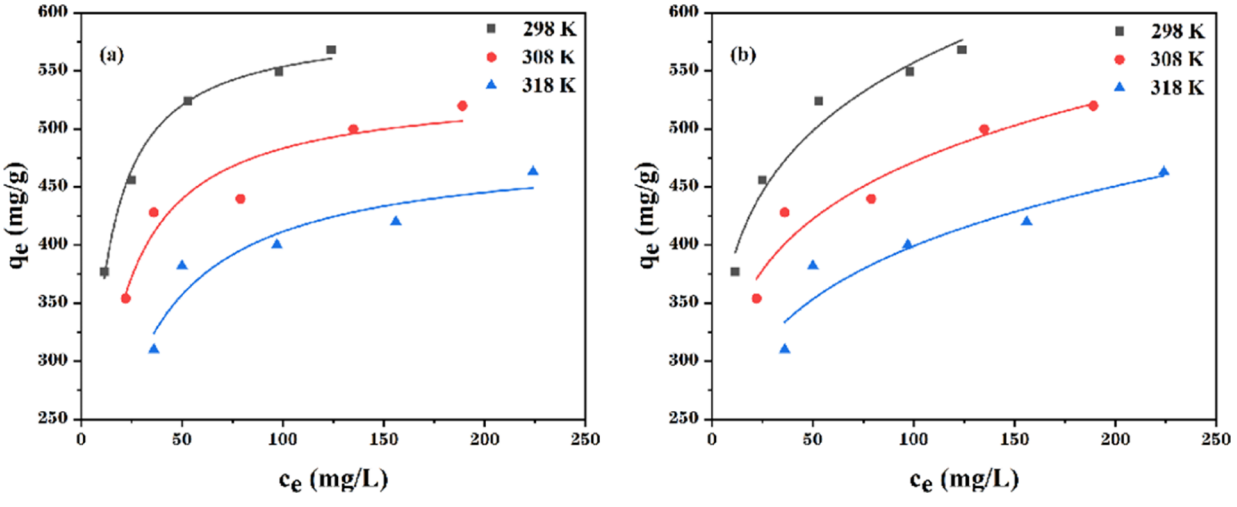

Figure 11. Isotherm plots of MB adsorption onto PUL/PAM/AC: (a) Langmuir isotherm and (b) Freundlich isotherm.

https://doi.org/10.1021/acsomega.2c06205
ACS Omega 2023, 8, 857−867

Table 1. Adsorption Isotherm Model Parameters for MB Absorbed by PUL/PAM/AC

models	parameters	298 K	308 K	318 K
Langmuir isotherm	q_m(mg·g^{-1})	591.4	536.5	485.1
	b (L·mg^{-1})	0.1464	0.09645	0.05541
	R^2	0.9971	0.9172	0.8912
Freundlich isotherm	K_f(mg$^{1-1/n}$·L$^{1/n}$·g^{-1})	265.6	226.8	177.8
	N	6.216	6.291	5.699
	R^2	0.9492	0.9032	0.8392

adsorption points on the surface of the medium. The formula is as follows[47]

$$q_e = K_f c_e^{1/n} \tag{5}$$

where K_f (mg$^{1-1/n}$·L$^{1/n}$·g^{-1}) and n are the experimental constants and surface inhomogeneity, respectively.

The adsorption isotherm model was fitted to better analyze the experiment. The results of adsorption models are shown in Figure 11, and the parameters are listed in Table 1. According to R^2 in the table, the adsorption of PUL/PAM/AC was more consistent with Langmuir model. In the table, the maximum adsorption capacity is 591.4 mg·g^{-1} at 298 K.

The specific parameters for comparing PUL/PAM/AC with other AC composites are shown in Table 2. PUL/PAM/AC gay friends have good adsorption prospects.

Table 2. Comparison of the Maximum Adsorption Capacity of Different Adsorbents

adsorbents	time (min)	q_m(mg·g^{-1})	T (K)	ref
alumina/AC	90	14.36	348	48
$CoFe_2O_4$/AC	40	120.4	298	49
chitosan/AC	120	143.5	323	50
Jengkol AC	300	170.9	303	51
PUL/PAM/AC	180	438.7	298	this work

Adsorption Kinetic Models. Adsorption kinetics is mainly used to study the adsorption velocity, reaction process, and reaction mechanism, which is of great significance to the study of adsorption process. The pseudo-first-order model is usually used to explain the liquid adsorption process, and the pseudo-second-order model can be used to think that the reaction is controlled by chemical action rather than physical migration.[24] The formulas are as follows

$$q_t = q_e(1 - e^{-kt}) \tag{6}$$

where k (min^{-1}) is the first-order adsorption rate constant

$$q_t = \frac{q_e^2 v_0 t}{1 + v_0 q_e t} \tag{7}$$

where v_0 (mg·g^{-1}·min^{-1}) is the adsorption rate without the adsorbent

$$q_t = k_i t^{1/2} + C_i \tag{8}$$

where K_i and C_i are, respectively, the diffusion rate constant (mg·g^{-1}·min$^{-1/2}$) and particle thickness constant (mg·g^{-1}).

Pseudo-first-order model, pseudo-second-order model, and intra-particle diffusion were used to fit the adsorption curve and analyze the adsorption process. The curve is shown in Figure 12, and the parameters and data are shown in Table 3.

Table 3. Fitting Results of MB Adsorption Kinetic Model Parameters on PUL/PAM/AC

model	parameters	values
pseudo-first-order model	q_e(mg·g^{-1})	488.8
	k (min^{-1})	0.06541
	R^2	0.9322
pseudo-second-order model	q_e(mg·g^{-1})	517.7
	v_0(mg·g^{-1}·min^{-1})	1.824
	R^2	0.9872
intra-particle diffusion model	C_1	8.351
	k_1(mg·g^{-1}·min$^{-1/2}$)	72.42
	R^2	0.9712
	C_2	418.1
	k_2(mg·g^{-1}·min$^{-1/2}$)	3.164
	R^2	0.8962

The determination coefficient R^2 of the surface kinetic model indicates that the adsorption conforms to the pseudo-second-order kinetic model. According to the diffusion model, the

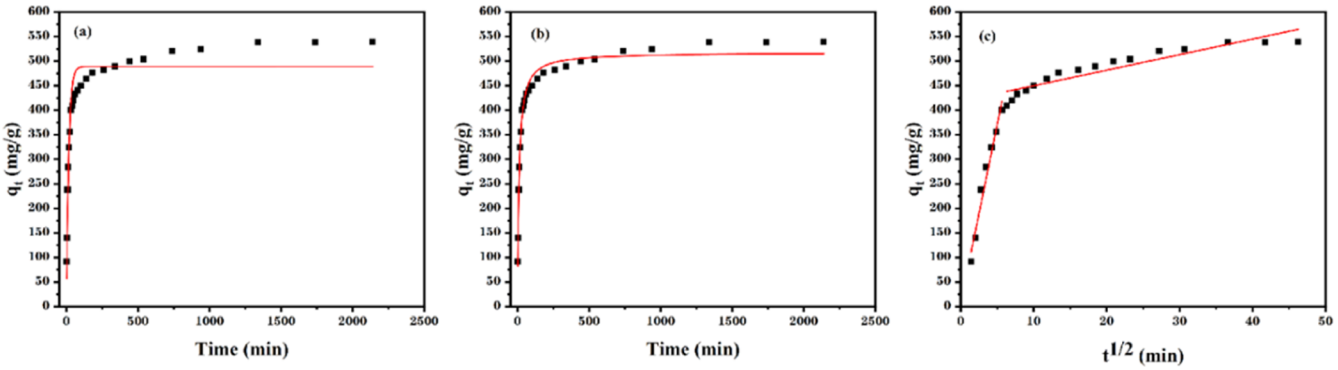

Figure 12. Pseudo-first-order model (a), pseudo-second-order model (b), and intra-particle diffusion model (c) for MB adsorption by PUL/PAM/AC.

https://doi.org/10.1021/acsomega.2c06205
ACS Omega 2023, 8, 857−867

adsorption process can comprise two stages. The large fitting slope of the first stage indicates the fast diffusion rate of the adsorbent boundary layer. The lower efficiency in the second stage corresponds to the lower diffusion rate in grains. The two-phase fitting lines were all at the origin, thus suggesting that the adsorption process is a complex one.

Adsorption Thermodynamic Models. The formula for further analysis of the adsorption process using the change of Gibbs free energy is as follows[52]

$$\Delta G = \Delta H - T\Delta S \tag{9}$$

$$\ln\left(\frac{q_e}{c_e}\right) = -\frac{\Delta H}{RT} + \frac{\Delta S}{R} \tag{10}$$

where ΔS, ΔH, ΔG, and R stand for the entropy change, enthalpy change, Gibbs-free-energy change, and universal gas constant (8.314 J·mol^{-1}·K^{-1}), respectively.

The data in Table 4 are thermodynamics-related parameters; ΔG is less than 0 at different temperatures, indicating that the reaction process was exothermic and spontaneous, and a higher temperature is not conducive to the adsorption process. The negative value of entropy ΔS indicates that the adsorption at the solid−liquid interface increases disordered.

Table 4. Thermodynamic Parameters for MB Adsorbed by PUL/PAM/AC

T (K)	ΔG(kJ·mol^{-1})	ΔS(kJ·mol^{-1}·K^{-1})	ΔH(J·mol^{-1}·K^{-1})
298	−9.242	−54.30	−153.2
308	−7.184		
318	−5.654		

Swelling Capacity of the Prepared Hydrogels at Different pH Levels. Figure 13 studies the swelling ratios of PUL/PAM and PUL/PAM/AC at different pH values. The swelling of PUL/PAM/AC is not significantly different from that of PUL/PAM, which can be attributed to the hydrogen bond formed between PUL and AC active groups to compensate for the hydrophilic property of the hydrogel. When the pH was 11, the curve has a rising trend because the −COOH group present in AC leads to the change of the overall −COOH contents, and the protonation and deprotonation of −COOH side groups on the hydrogel chain in acidic and alkaline environments are the main reasons for the change of swelling properties.[53]

Mechanical Strength of PUL/PAM/AC. Figure 14 shows the mechanical tensile properties of PUL/PAM/AC composite hydrogels with different AC content ratios. As indicated by the above result, with the increase of dosage of AC, tensile strength and the maximum strain increase gradually, mainly attributed to the active group on the AC and PUL on the carboxyl strong hydrogen bond interaction, which can facilitate the load transfer between polymer molecular chains. Besides, AC had high strength and a high modulus, thus effectively improving the mechanical properties of the hydrogel. With the increase of AC to the ratio of 8:1, the tensile strength and maximum strain began to decrease slowly. The possible reason for this result is that AC strengthened the ternary polymerization network structure, resulting in AC agglomeration, which reduced the interface bonding force between hydrogels and thus reduced the mechanical properties.[54]

Adsorption Mechanism. The adsorption process of PUL/PAM/AC is shown in Figure 15. The high adsorption capacity of PUL/PAM/AC terpolymer hydrogel for MB depends on the internal fold structure and abundant functional groups on the surface. The adsorption process is mainly completed in three forms: through electrostatic attraction with MB, carboxyl group with MB molecule bonding hydrogen bond, and $\pi-\pi$ stacking between benzene rings.

CONCLUSIONS

In this study, the synthesis, characterization, and adsorption of PUL/PAM/AC hydrogel composites were described. In the experiment, PAM was used as a tough hydrogel matrix, and the excellent biocompatibility and stability of PUL were adopted to enhance the mechanical strength of the hydrogel and the adsorption capacity of AC, providing more active sites and promoting the adsorption process. The experimental data fully indicated that the maximum adsorption capacity is 591.4 mg·g^{-1} at a temperature of 298 K, pH 10, and a PUL:AC ratio of 6:1. The swelling properties and mechanical strength of the composite hydrogels showed that the composite hydrogels with AC exhibited better hydrophilic and swelling properties and improved the tensile strength and maximum expansion in a certain range. The characterization result verified that the hydrogel exhibits a rich layered fold structure, good thermal

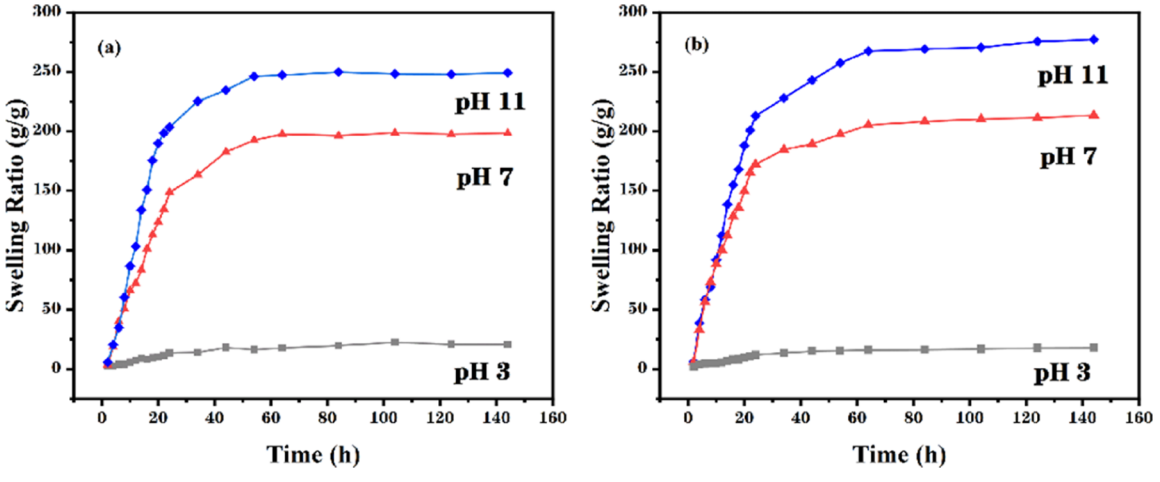

Figure 13. Comparison of swelling ratio of (a) PUL/PAM and (b) PUL/PAM/AC at different pH.

https://doi.org/10.1021/acsomega.2c06205
ACS Omega 2023, 8, 857−867

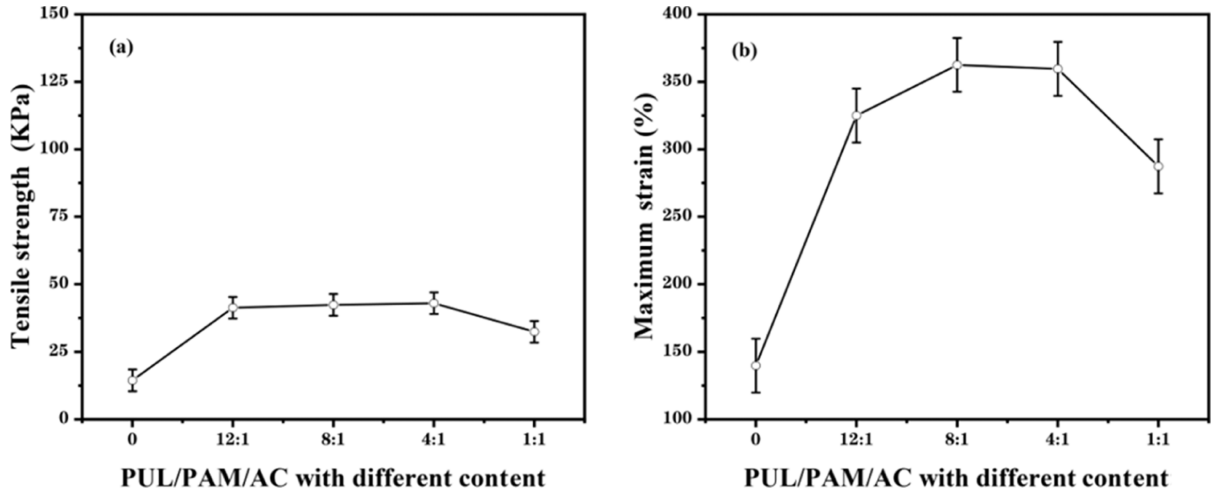

Figure 14. Influence of different AC content ratios on tensile strength (a) and strain properties of PUL/PAM/AC composite hydrogel (b).

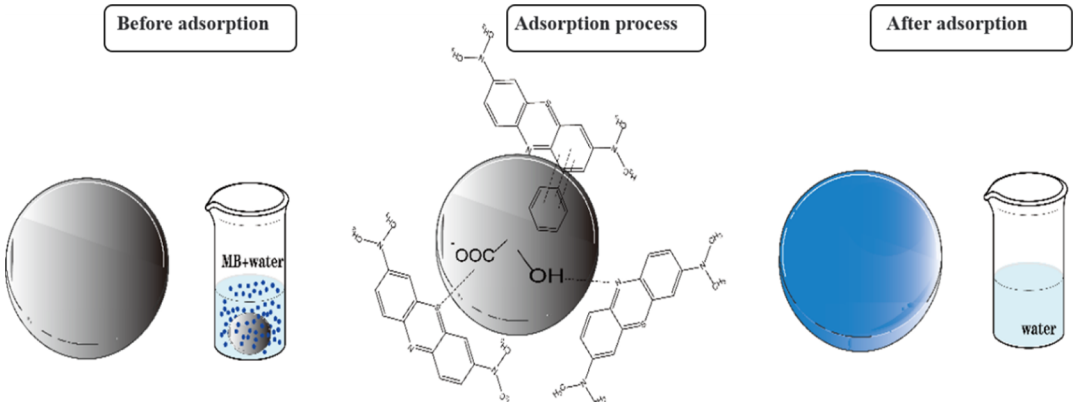

Figure 15. Adsorption mechanism of PUL/PAM/AC for MB.

stability, and high adsorption capacity. The adsorption of MB conforms to pseudo-first-order kinetics and Langmuir isotherms. In this study, an environment-friendly, cheap, simple, and efficient way was presented for the composite hydrogel in the direction of water treatment. This study provides an environment-friendly, cheap, simple, and efficient composite hydrogel for the treatment of dye contamination.

AUTHOR INFORMATION

Corresponding Author

Yanhui Li − *College of Mechanical and Electrical Engineering, Qingdao University, Qingdao 266071, China; Laboratory of Fiber Materials and Modern Textile, The Growing Base for State Key Laboratory, Qingdao University, Qingdao 266071, China;* orcid.org/0000-0001-7370-0233; Email: liyanhui537@163.com

Authors

Kewei Chen − *College of Mechanical and Electrical Engineering, Qingdao University, Qingdao 266071, China*

Mingzhen Wang − *College of Mechanical and Electrical Engineering, Qingdao University, Qingdao 266071, China*

Qiuju Du − *Laboratory of Fiber Materials and Modern Textile, The Growing Base for State Key Laboratory, Qingdao University, Qingdao 266071, China*

Yaohui Sun − *College of Mechanical and Electrical Engineering, Qingdao University, Qingdao 266071, China*

Yang Zhang − *College of Mechanical and Electrical Engineering, Qingdao University, Qingdao 266071, China*

Bing Chen − *College of Mechanical and Electrical Engineering, Qingdao University, Qingdao 266071, China*

Zhenyu Jing − *College of Mechanical and Electrical Engineering, Qingdao University, Qingdao 266071, China*

Yonghui Jin − *College of Mechanical and Electrical Engineering, Qingdao University, Qingdao 266071, China*

Shiyong Zhao − *College of Mechanical and Electrical Engineering, Qingdao University, Qingdao 266071, China*

Complete contact information is available at: https://pubs.acs.org/10.1021/acsomega.2c06205

Notes

The authors declare no competing financial interest.

ACKNOWLEDGMENTS

The authors are grateful to the National Natural Science Foundation of China (51672140) and the Taishan Scholar Project of Shandong Province (201511029).

REFERENCES

(1) Liu, S.; Ge, H.; Wang, C.; Zou, Y.; Liu, J. Agricultural waste/graphene oxide 3D bio-adsorbent for highly efficient removal of methylene blue from water pollution. *Sci. Total Environ.* **2018**, *628−629*, 959−968.

(2) Kavil, Y. N.; Shaban, Y. A.; Alelyani, S. S.; Al-Farawati, R.; Orif, M. I.; Ghandourah, M. A.; Schmidt, M. r.; Turki, A. J.; Zobidi, M. The removal of methylene blue as a remedy of dye-based marine pollution: a photocatalytic perspective. *Res. Chem. Intermed.* **2020**, *46*, 755−768.
(3) Rafatullah, M.; Sulaiman, O.; Hashim, R.; Ahmad, A. Adsorption of methylene blue on low-cost adsorbents: A review. *J. Hazard. Mater.* **2010**, *177*, 70−80.
(4) Chia, C.-h.; Razali, N. F.; Sajab, M. S.; Zakaria, S.; Huang, N. M.; Lim, H. N. Methylene Blue Adsorption on Graphene Oxide. *Sains Malays.* **2013**, *42*, 819−826.
(5) Ghosh, D.; Bhattacharyya, K. G. Adsorption of methylene blue on kaolinite. *Appl. Clay Sci.* **2002**, *20*, 295−300.
(6) Kheradmand, A.; Negarestani, M.; Kazemi, S.; Shayesteh, H.; Javanshir, S.; Ghiasinejad, H. Adsorption behavior of rhamnolipid modified magnetic Co/Al layered double hydroxide for the removal of cationic and anionic dyes. *Sci. Rep.* **2022**, *12*, 14623.
(7) Kheradmand, A.; Negarestani, M.; Mollahosseini, A.; Shayesteh, H.; Farimaniraad, H. Low-cost treated lignocellulosic biomass waste supported with FeCl3/Zn(NO3)(2) for water decolorization. *Sci. Rep.* **2022**, *12*, 16442.
(8) Lee, A. L. Z.; Ng, V. W. L.; Gao, S.; Hedrick, J. L.; Yang, Y. Y. Injectable Biodegradable Hydrogels from Vitamin D-Functionalized Polycarbonates for the Delivery of Avastin with Enhanced Therapeutic Efficiency against Metastatic Colorectal Cancer. *Biomacromolecules* **2015**, *16*, 465−475.
(9) Yue, K.; Trujillo-de Santiago, G.; Alvarez, M.; Tamayol, A.; Annabi, N.; Khademhosseini, A. Synthesis, properties, and biomedical applications of gelatin methacryloyl (GelMA) hydrogels. *Biomaterials* **2015**, *73*, 254−271.
(10) Guenther, M.; Gerlach, G.Hydrogels for Chemical Sensors. In *Hydrogel Sensors and Actuators: Engineering and Technology*; Gerlach, G., Arndt, K. F., Eds.; Springer Nature, 2009; Vol. *6*, pp 165−195.
(11) Bai, X.; Gao, M.; Syed, S.; Zhuang, J.; Xu, X.; Zhang, X.-Q. Bioactive hydrogels for bone regeneration. *Bioact. Mater.* **2018**, *3*, 401−417.
(12) Samadian, H.; Maleki, H.; Allahyari, Z.; Jaymand, M. Natural polymers-based light-induced hydrogels: Promising biomaterials for biomedical applications. *Coord. Chem. Rev.* **2020**, *420*, 213432.
(13) Trieu, H. H.; Qutubuddin, S. Polyvinyl alcohol hydrogels I. Microscopic structure by freeze-etching and critical point drying techniques. *Colloid Polym. Sci.* **1994**, *272*, 301−309.
(14) Huang, T.; Xu, H.; Jiao, K.; Zhu, L.; Brown, H. R.; Wang, H. A novel hydrogel with high mechanical strength: A macromolecular microsphere composite hydrogel. *Adv. Mater.* **2007**, *19*, 1622−1626.
(15) Katoch, A.; Choudhury, A. R. Understanding the rheology of novel guar-gellan gum composite hydrogels. *Mater. Lett.* **2020**, *263*, 127234.
(16) Taşdelen, B.; Çifçi, D. I.; Meriç, S. Preparation and characterization of chitosan/AMPS/kaolinite composite hydrogels for adsorption of methylene blue. *Polym. Bull.* **2022**, *79*, 9643.
(17) Zhang, D.; Cai, J.; Xu, W.; Dong, Q.; Li, Y.; Liu, G.; Wang, Z. Synthesis,characterization and adsorption property of cellulose nanofiber-based hydrogels. *J. Forestry Eng.* **2019**, *4*, 92−98.
(18) Ge, H. Y.; Wang, C. C.; Liu, S. S.; Huang, Z. Synthesis of citric acid functionalized magnetic graphene oxide coated corn straw for methylene blue adsorption. *Bioresour. Technol.* **2016**, *221*, 419−429.
(19) Abed, A.; Assoul, N.; Ba, M.; Derkaoui, S. M.; Portes, P.; Louedec, L.; Flaud, P.; Bataille, I.; Letourneur, D.; Meddahi-Pellé, A. Influence of polysaccharide composition on the biocompatibility of pullulan/dextran-based hydrogels. *J. Biomed. Mater. Res., Part A* **2011**, *96*, 535−542.
(20) Wong, V. W.; Rustad, K. C.; Glotzbach, J. P.; Sorkin, M.; Inayathullah, M.; Major, M. R.; Longaker, M. T.; Rajadas, J.; Gurtner, G. C. Pullulan Hydrogels Improve Mesenchymal Stem Cell Delivery into High-Oxidative-Stress Wounds. *Macromol. Biosci.* **2011**, *11*, 1458−1466.
(21) Zhang, L.; Liu, J.; Zheng, X.; Zhang, A.; Zhang, X.; Tang, K. Pullulan dialdehyde crosslinked gelatin hydrogels with high strength for biomedical applications. *Carbohydr. Polym.* **2019**, *216*, 45−53.
(22) Gonçalves, J. O.; da Silva, K. A.; Rios, E. C.; Crispim, M. M.; Dotto, G. L.; de Almeida Pinto, L. A. Single and Binary Adsorption of Food Dyes on Chitosan/Activated Carbon Hydrogels. *Chem. Eng. Technol.* **2019**, *42*, 454−464.
(23) Qiu, J.; Xu, L.; Peng, J.; Zhai, M.; Zhao, L.; Li, J.; Wei, G. Effect of activated carbon on the properties of carboxymethylcellulose/activated carbon hybrid hydrogels synthesized by γ-radiation technique. *Carbohydr. Polym.* **2007**, *70*, 236−242.
(24) Hameed, B. H.; Din, A. T. M.; Ahmad, A. L. Adsorption of methylene blue onto bamboo-based activated carbon: Kinetics and equilibrium studies. *J. Hazard. Mater.* **2007**, *141*, 819−825.
(25) Darnell, M. C.; Sun, J.-Y.; Mehta, M.; Johnson, C.; Arany, P. R.; Suo, Z.; Mooney, D. J. Performance and biocompatibility of extremely tough alginate/polyacrylamide hydrogels. *Biomaterials* **2013**, *34*, 8042−8048.
(26) Gao, G.; Du, G.; Sun, Y.; Fu, J. Self-Healable, Tough, and Ultrastretchable Nanocomposite Hydrogels Based on Reversible Polyacrylamide/Montmorillonite Adsorption. *ACS Appl. Mater. Interfaces* **2015**, *7*, 5029−5037.
(27) Liu, R.; Liang, S.; Tang, X.-Z.; Yan, D.; Li, X.; Yu, Z.-Z. Tough and highly stretchable graphene oxide/polyacrylamide nanocomposite hydrogels. *J. Mater. Chem.* **2012**, *22*, 14160−14167.
(28) Sonmez, B.; Celikkol, A. N. Pullulan based hydrogels for the removal of various metal ions from aqueous solutions. *J. Environ. Chem. Eng.* **2021**, *9*, 106188.
(29) Chen, B.; Li, Y.; Li, M.; Cui, M.; Xu, W.; Li, L.; Sun, Y.; Wang, M.; Zhang, Y.; Chen, K. Rapid adsorption of tetracycline in aqueous solution by using MOF-525/graphene oxide composite. *Microporous Mesoporous Mater.* **2021**, *328*, 111457.
(30) Xu, W.; Li, Y.; Wang, H.; Du, Q.; Li, M.; Sun, Y.; Cui, M.; Li, L. Study on the Adsorption Performance of Casein/Graphene Oxide Aerogel for Methylene Blue. *ACS Omega* **2021**, *6*, 29243−29253.
(31) Hernandez-Martínez, A. R.; Lujan-Montelongo, J. A.; Silva-Cuevas, C.; Mota-Morales, J. D.; Cortez-Valadez, M.; Ruíz-Baltazar, A.; Cruz, M.; Herrera-Ordonez, J. Swelling and methylene blue adsorption of poly(N,N-dimethylacrylamide-co-2-hydroxyethyl methacrylate) hydrogel. *React. Funct. Polym.* **2018**, *122*, 75−84.
(32) Bao, Y.; Ma, J. Z.; Li, N. Synthesis and swelling behaviors of sodium carboxymethyl cellulose-g-poly(AA-co-AM-co-AMPS)/MMT superabsorbent hydrogel. *Carbohydr. Polym.* **2011**, *84*, 76−82.
(33) Zhu, H. J.; Jia, Y. F.; Wu, X.; Wang, H. Removal of arsenic from water by supported nano zero-valent iron on activated carbon. *J. Hazard. Mater.* **2009**, *172*, 1591−1596.
(34) Qi, X.; Zeng, Q.; Tong, X.; Su, T.; Xie, L.; Yuan, K.; Xu, J. X.; Shen, J. L. Polydopamine/montmorillonite-embedded pullulan hydrogels as efficient adsorbents for removing crystal violet. *J. Hazard. Mater.* **2021**, *402*, 123359.
(35) Anirudhan, T. S.; Suchithra, P. S.; Rijith, S. Amine-modified polyacrylamide-bentonite composite for the adsorption of humic acid in aqueous solutions. *Colloids Surf., A* **2008**, *326*, 147−156.
(36) Suhas; Carrott, P. J. M.; Ribeiro Carrott, M. M. L. R. Lignin - from natural adsorbent to activated carbon: A review. *Bioresour. Technol.* **2007**, *98*, 2301−2312.
(37) Su, T.; Wu, L. P.; Pan, X. H.; Zhang, C.; Shi, M. Y.; Gao, R. R.; Qi, X. L.; Dong, W. Pullulan-derived nanocomposite hydrogels for wastewater remediation: Synthesis and characterization. *J. Colloid Interface Sci.* **2019**, *542*, 253−262.
(38) Dittmann, D.; Braun, U.; Jekel, M.; Ruhl, A. S. Quantification and characterisation of activated carbon in activated sludge by thermogravimetric and evolved gas analyses. *J. Environ. Chem. Eng.* **2018**, *6*, 2222−2231.
(39) Tang, F.; Yu, H.; Abdalkarim, S. Y. H.; Sun, J.; Fan, X.; Li, Y.; Zhou, Y.; Tam, K. C. Green acid-free hydrolysis of wasted pomelo peel to produce carboxylated cellulose nanofibers with super absorption/flocculation ability for environmental remediation materials. *Chem. Eng. J.* **2020**, *395*, 125070.
(40) Li, Y.; Du, Q.; Liu, T.; Peng, X.; Wang, J.; Sun, J.; Wang, Y.; Wu, S.; Wang, Z.; Xia, Y.; Xia, L. Comparative study of methylene

https://doi.org/10.1021/acsomega.2c06205
ACS Omega 2023, 8, 857−867

blue dye adsorption onto activated carbon, graphene oxide, and carbon nanotubes. *Chem. Eng. Res. Des.* **2013**, *91*, 361−368.
(41) Chen, L.; Li, Y.; Hu, S.; Sun, J.; Du, Q.; Yang, X.; Ji, Q.; Wang, Z.; Wang, D.; Xia, Y. Removal of methylene blue from water by cellulose/graphene oxide fibres. *J. Exp. Nanosci.* **2016**, *11*, 1156−1170.
(42) Almeida, C. A. P.; Debacher, N. A.; Downs, A. J.; Cottet, L.; Mello, C. A. D. Removal of methylene blue from colored effluents by adsorption on montmorillonite clay. *J. Colloid Interface Sci.* **2009**, *332*, 46−53.
(43) Fan, S.; Wang, Y.; Wang, Z.; Tang, J.; Tang, J.; Li, X. Removal of methylene blue from aqueous solution by sewage sludge-derived biochar: Adsorption kinetics, equilibrium, thermodynamics and mechanism. *J. Environ. Chem. Eng.* **2017**, *5*, 601−611.
(44) Senthilkumaar, S.; Varadarajan, P. R.; Porkodi, K.; Subbhuraam, C. Adsorption of methylene blue onto jute fiber carbon: kinetics and equilibrium studies. *J. Colloid Interface Sci.* **2005**, *284*, 78−82.
(45) Potgieter, J. H. Adsorption of methylene blue on activated carbon: An experiment illustrating both the Langmuir and Freundlich isotherms. *J. Chem. Educ.* **1991**, *68*, 349−350.
(46) Abadian, S.; Shayesteh, H.; Rahbar-Kelishami, A. Effective adsorption of diclofenac sodium from aqueous solution using cationic surfactant modified Cuminum cyminum agri-waste: kinetic, equilibrium, and thermodynamic studies. *Int. J. Phytorem.* **2022**, DOI: 10.1080/15226514.2022.2113367.
(47) Ahmed, M. J.; Dhedan, S. K. Equilibrium isotherms and kinetics modeling of methylene blue adsorption on agricultural wastes-based activated carbons. *Fluid Phase Equilib.* **2012**, *317*, 9−14.
(48) Hariani, P. L.; Muryati; FatmaIop In Synthesis Alumina-Activated Carbon Composite Using Sol-Gel Method As Adsorption for Methylene Blue Dye. In *6th International Conference of the Indonesian-Chemical-Society (ICIC), Palembang, Indonesia, Oct 17−18, 2018*: Palembang, Indonesia, 2017.
(49) Ai, L.; Jiang, J.; Tang, J. Preparation of Activated Carbon/CoFe2O4 Composite and Its Adsorption Properties for Methylene Blue. *Chin. J. Appl. Chem.* **2010**, *27*, 710−715.
(50) Marrakchi, F.; Ahmed, M. J.; Khanday, W. A.; Asif, M.; Hameed, B. H. Mesoporous-activated carbon prepared from chitosan flakes via single-step sodium hydroxide activation for the adsorption of methylene blue. *Int. J. Biol. Macromol.* **2017**, *98*, 233−239.
(51) Mohd Ramli, M. R.; Shoparwe, N. F.; Ahmad, M. A. Methylene Blue Removal Using Activated Carbon Adsorbent from Jengkol Peel: Kinetic and Mass Transfer Studies. *Arabian J. Sci. Eng.* **2022**, DOI: 10.1007/s13369-022-07141-5.
(52) Mohammed, N.; Lian, H.; Islam, M. S.; Strong, M.; Shi, Z. Q.; Berry, R. M.; Yu, H. Y.; Tam, K. C. Selective adsorption and separation of organic dyes using functionalized cellulose nanocrystals. *Biochem. Eng. J.* **2021**, *417*, 129237.
(53) Singh, R.; Pal, D.; Mathur, A.; Singh, A.; Krishnan, M. A.; Chattopadhyay, S. An efficient pH sensitive hydrogel, with biocompatibility and high reusability for removal of methylene blue dye from aqueous solution. *React. Funct. Polym.* **2019**, *144*, 104346.
(54) Niu, J. B.; Wang, J. Q.; Dai, X. F.; Shao, Z. Q.; Huang, X. N. Dual physically crosslinked healable polyacrylamide/cellulose nanofibers nanocomposite hydrogels with excellent mechanical properties. *Carbohydr. Polym.* **2018**, *193*, 73−81.

https://doi.org/10.1021/acsomega.2c06205
ACS Omega 2023, 8, 857−867